



This is a repository copy of *A Macroscopic Transport Problem*.

White Rose Research Online URL for this paper:
<http://eprints.whiterose.ac.uk/85728/>

Monograph:

Dash, I. and Rose, E. (1976) *A Macroscopic Transport Problem*. Research Report. ACSE Research Report 44 . Department of Automatic Control and Systems Engineering

Reuse

Unless indicated otherwise, fulltext items are protected by copyright with all rights reserved. The copyright exception in section 29 of the Copyright, Designs and Patents Act 1988 allows the making of a single copy solely for the purpose of non-commercial research or private study within the limits of fair dealing. The publisher or other rights-holder may allow further reproduction and re-use of this version - refer to the White Rose Research Online record for this item. Where records identify the publisher as the copyright holder, users can verify any specific terms of use on the publisher's website.

Takedown

If you consider content in White Rose Research Online to be in breach of UK law, please notify us by emailing eprints@whiterose.ac.uk including the URL of the record and the reason for the withdrawal request.



eprints@whiterose.ac.uk
<https://eprints.whiterose.ac.uk/>

Q 629-8(S)

~~AMF 507~~

UNIVERSITY OF SHEFFIELD
Department of Control Engineering

A MACROSCOPIC TRANSPORT PROBLEM



I. Dash and E. Rose

Research Report No. 44

April 1976

P 59341
22 11 77

SHEFFIELD UNIT
APPLIED SCIENCE
LIBRARY

A MACROSCOPIC TRANSPORT PROBLEM

Abstract

An analytical approach is used to investigate the process of iron ore sintering which represents a problem in macroscopic transport and as such, the approach used may be of value to other workers concerned with modelling processes involving gas-solid and gas-liquid energy and mass transfer.

The paper discusses the formulation and simulation of the process equations. The results of a simulation exercise are compared with those obtained from tests on pilot plant to establish the validity of the model. The effects of ignition time, ignition temperature, size of mix, coke content, water content and ore density on heat wave propagation are then investigated.

(i)

NOTATION

- a Specific surface area $\{m^2/m^3(\text{bed})\}$. In the case of spherical particles in a packed bed $a = 6(1-\epsilon)/d_p$.
- $C_{CO_2}, C_{N_2}, C_{O_2}$ Concentrations of CO_2, N_2 and O_2 in gas (mol/m^3)
- $C_{CO_2}^*, C_{N_2}^*, C_{O_2}^*$ Concentrations of CO_2, N_2 and O_2 in gas at $0^\circ C$ (mol/m^3)
- C_g, C_p Specific heats of gases and solid particles ($J/Kg^\circ C$)
- D Diffusion coefficient (m^2/s)
- D_{ON} Diffusion coefficient of O_2 through N_2 (m^2/s)
- d_p Average diameter of solid particles (m)
- F_u Heat available for fusion (J)
- G Mass velocity of gas ($Kg/m^2 s$)
- H_c Heat of combustion of coke $\{J/g\text{-atom}(c)\}$.
- H_v Latent heat of vaporization of water (J/Kg)
- h Depth of bed (m)
- h_p Convective heat transfer coefficient between solid particles and gas ($J/m^2 s^\circ C$)
- K Overall combustion rate constant (m/s)
- K_c Chemical combustion rate constant (m/s)
- K_g Thermal conductivity of the gas ($J/m s^\circ C$)
- K_m Mass transfer coefficient (m/s)
- K_p Thermal conductivity of solid particles ($J/m s^\circ C$)
- n_c Number of coke particles per unit volume of the bed $\{1/m^3(\text{bed})\}$
- N_u Nussett number (-)
- P_r Prandtl number (-)
- R Universal gas constant ($J/mol^\circ K$)
- R_c Overall reaction rate of coke in the bed $\{g\text{-atom}(C)/s m^3(\text{bed})\}$
- R_e Reynolds number (-)
- r_c Radius of coke (m)
- S_c Schmidt number (-)
- S_h Sherwood number (-)
- t Temperature of solid particles ($^\circ K$)
- T_F Fusion temperature ($^\circ K$)

(ii)

- W Humidity of the gas {Kg /Kg (dry gas)}
- Δz Width of zones into which the bed is divided during simulation (m)
- z Downward distance from the surface of the bed (m)
- ϵ Voidage (-)
- θ Time (s)
- λ Thermal conductivity of gas (J/m s^oC)
- μ Viscosity of gas (Kg / ms)
- ρ_p Density of sinter materials (Kg /m³)
- ρ_g Density of gas (Kg /m³)
- τ Temperature of gas (^oK)
- $\Delta\phi$ Update period for simulation (s)

INTRODUCTION

A common method of producing sinter from iron ore involves the use of a Dwight-Lloyd sinter strand. The sinter strand may be regarded as a continuous moving grate which is loaded with a raw mixture of ore, coke and water to form a bed. Situated below the bed there is a series of wind-boxes which allows a large fan to suck air downwards through the bed. The material is ignited as it passes under an ignition hood at the beginning of the strand and a heat wave gradually passes down through the bed at a rate which causes burnthrough to occur at the output end of the strand. The effect of the heat wave is to drive off the volatiles and agglomerate the mixture to form sinter. For optimum working conditions both sinter quality and plant output must be maximised. The maximum plant output for any given suction across the bed occurs when the burnthrough point of the heat wave is at the end of the strand. Thus the influence of the process variables on sinter quality and the rate of heat wave propagation should be known so that satisfactory operating conditions may be chosen. The sinter bed may be regarded as a series of vertically divided sections each moving horizontally along the strand. The temperature history of one such section from ignition to burnthrough is representative of the whole bed and is obtained in practice by the use of pilot plant in the form of a sinter test-pot. A test-pot provides a realistic but limited facility for the practical analysis of the sintering process, since a change in a controlled variable simultaneously changes a number of fundamental process variables. It is therefore difficult to establish from test-pot data the significance of individual process variables. A digital simulation of a test-pot process is not, however, similarly limited as it enables the influence of individual process variables to be readily investigated.

Initially, the paper briefly outlines the physical relationships on which sintering is dependant. Obviously, it is impracticable to include all the relationships within an analytical model and so only those relationships

which in the authors' views are important are included in the model discussed here. The next part of the paper explains the technique used to solve the non-linear partial differential and algebraic equations describing the process. A comparison is then made between the results of the digital simulation and actual test-pot data to show that the simulation results are satisfactory.

The final part of the paper is devoted to an investigation of the effects of individual process variables on sinter quality and heat wave propagation.

FUNDAMENTAL SINTER BED EQUATIONS

Mass and Energy Balance Equations

Although the aim is to derive a set of analytical equations describing the sintering process, several empirical assumptions must be made where insufficient information exists for an analytical approach to be made. The sintering process may be studied by assuming a zonal structure, Fig. 1. The zones chosen are fairly arbitrary and in practice overlap. The approach adopted is to solve all equations simultaneously, permitting combustion to die out naturally as all the carbon particles react. The 'zones' thus develop from the equations rather than being imposed as a prerequisite of the model.

The overall combustion rate of coke particles is dependant upon both chemical and mass transfer because before combustion of coke can occur oxygen has to diffuse up to the coke particle surface. The overall combustion rate is given by:-

$$R_c = 4\pi r_c^2 n_c K C_{O_2} \dots\dots\dots (1)$$

where $4\pi r_c^2$ = surface area of coke particles

n_c = number of coke particles per unit volume

and

$$K = \frac{K_c \cdot K_m}{K_c + K_m}$$

K_m is the coefficient of mass transfer,

K_c is the chemical combustion rate constant.

Using basic chemical engineering principles, the following equations for the heating, cooling and combustion zones have been derived {1,2};

Mass velocity of gas through bed:-

$$G = \epsilon \cdot \rho_g \cdot (\partial z / \partial \theta) \quad \dots\dots(2)$$

The energy balance equation for the gas passing through the bed is:-

$$G \{ \partial(C_g \tau) / \partial z \} + \epsilon \rho_g \{ \partial(C_g \tau) / \partial \theta \} + h_p a(\tau - t) = 0 \quad \dots(3)$$

bulk convection accumulation in gas convection exchange to solid

An equivalent equation for the solid is:-

$$(1-\epsilon) \rho_p \{ \partial(C_p t) / \partial \theta \} + h_p a(t - \tau) + H_c \cdot R_c = 0 \quad \dots(4)$$

accumulation in solid convection exchange to gas heat from reactions in solid

The following equations represent the mass balance of O_2 in the gas phase;

$$\partial(GC_{O_2} / \rho_g) / \partial z + \partial(\epsilon C_{O_2}) / \partial \theta + R_c = 0 \quad \dots\dots\dots(5)$$

bulk convection accumulation in gas net change in O_2 by reaction

where

$$C_{O_2} + C_{CO_2} + C_{N_2} = 44.6 (273/\tau) \quad \dots\dots\dots(6)$$

and

$$\rho_g = (32 C_{O_2}^* + 44 C_{CO_2}^* + 28 C_{N_2}^*) \cdot 10^{-3} \cdot (273/\tau) \quad \dots\dots\dots(7)$$

The assumptions made in formulating equations (1) to (7) are:-

- (1) Gas flow is one-dimensional (If the diameter of the particles in a stable granular bed is less than thirty times the bed diameter, piston flow can be assumed).
- (2) Gas species are ideal.
- (3) Eddy diffusion effects are small and can be ignored.
- (4) System is adiabatic.

- (5) Radiative effects within the gas and between the gas and solid are insignificant.
- (6) The reaction of coke with oxygen takes place on the surface of the coke particle and not in the gas.
- (7) The inside temperature of a solid particle is identical to its surface temperature.

Preliminary investigations show that convective heat transfer is the major factor promoting heat wave propagation and that for the gas the axial heat conduction and enthalpy of gas from the solid can be ignored. Similarly, axial heat conduction and radiation from solid to solid may be left out of the solid energy balance equation.

Drying and Condensation

Although it is possible to formulate energy and mass balance equations for the drying zones, both falling and constant rate, it proved to be impractical to implement the equations and a simpler approach was used.

The main reasons for the impracticality of the analytical approach were:-

- (1) No data could be found for the proportions of water dried during the constant rate period and the first falling rate period.
- (2) The rate constant for drying at the front edge of the heat wave was of the same order of magnitude as the update period of the simulation, hence a detailed investigation would have necessitated the use of smaller time increments and hence slowed down the computation of the solution. The removal of water during sintering accounts for only about 10% of the available energy, hence a less accurate representation does not significantly affect the overall solution.

Representation of the drying phase was therefore implemented by assuming that all evaporation occurred at 100°C , the expression for evaporation being:-

$$\text{heat from gas} = (\text{water evaporated}) \times (\text{latent heat of vaporization})$$

As the gas passes down the bed laden with moisture from the drying zone it cools until it reaches the dewpoint. At the dewpoint, the moisture

condenses and the bed temperature rises. Using this approach, the raw mix below the combustion and heating zones gradually rises in temperature until it is all at the dewpoint temperature. Using a least squares curve -fitting technique and graphical data given by Perry (4) the relationship between dewpoint temperature τ_{DEW} and moisture content was found to be approximately

$$\tau_{DEW} = 293.4 + 324.6 W - 594.1 W^2 + 292.1 W^3 \dots\dots\dots (8)$$

The equation for the heat gained by the bed due to condensation is:-

$$\text{heat to bed} = (\text{mass of water condensed}) \times (\text{latent heat of condensation})$$

Fusion and Limestone Reduction

The set of equations (2-7) excluded limestone reduction (limestone is contained in self-fluxing sinters) and fusion, both of which need to be included in a realistic model of the sintering process.

Purely analytical modelling of the fusion process is extremely complex, particularly for self-fluxing sinter. Work reported by Nyquist (5) and Price et al(6) on practical investigations illustrates the difficulty of predicting mineralogy changes due to fusion. To avoid this problem the assumption is made that when a bed temperature is reached corresponding to the maximum temperature obtained from test rig results, the excess energy is used in fusion. This assumption is founded on the fact that the maximum temperature achieved in practice is reasonably independent of coke content for high quality self-fluxing mixes containing hematite and magnetite. The majority of sintering mixes are of this type. In the model the heat is stored until cooling occurs behind the combustion zone. The results of a simulation exercise in which the above assumptions were made, agree with the results of tests on pilot plant.

Limestone reduction accounts for only about 5% of the available energy and therefore has little effect on the temperature profile. At present, limestone reduction is built into the model as a simple endothermic reaction

The expressions for most of the important terms used in the previous equations, e.g. chemical combustion rate of coke, specific heats of solids and gas, are given in Appendix I.

METHOD OF SIMULATION

The energy balance equation for the gas phase passing through the bed and the equivalent equation for the solid are:-

$$G\{\partial(C_g \tau)/\partial z\} + \epsilon \rho_g \{\partial(C_g \tau)/\partial \theta\} + h_p a.(\tau-t) = 0 \dots\dots\dots (9)$$

and

$$(1-\epsilon)\rho_p \{\partial(C_p t)/\partial \theta\} + h_p a (t-\tau) + H_c.R_c = 0 \dots\dots\dots(10)$$

Now for the case of convective heat transfer only, without limestone, drying, combustion and fusion. The method of solution is to assume that the test-pot may be vertically divided into n zones. The thickness of the ith zone is Δz_i and the total bed thickness is therefore $\sum_1^n \Delta z_i$.

The above equations may be simplified by substituting for C_g and C_p from equations given in Appendix I.

$$\therefore G.B_g . \partial\tau/\partial z + \epsilon \rho_g .B_g . \partial\tau/\partial \theta + h_p a (\tau-t) = 0 \dots\dots(11)$$

and

$$(1-\epsilon)\rho_p .B_s . \partial t/\partial \theta + h_p a (t-\tau) = 0 \dots\dots\dots(12)$$

where

$$B_g = 881.0 + 0.62\tau - 2.37 \cdot 10^{-4} \cdot \tau^2 \dots\dots\dots(13)$$

and

$$B_s = 753.0 + 0.26t \dots\dots\dots(14)$$

Consider a narrow band of hot gas passing through the bed. Due to the very large difference in density of the solid and gas (approx. 3000 :1), the change in temperature of the solid during the period which the gas takes to pass through it is negligible. The gas temperature, however, changes quite significantly. The temperature of a band of gas of thickness δz , where δz is very small, may be repeatedly calculated as the band passes through the bed.

During transit time the solid temperatures $t_1 \dots t_n$ are assumed constant.

The transit time through the i^{th} zone of thickness Δz_i is given by:-

$$\Delta\theta_i = \frac{\epsilon \cdot \rho_g \Delta z_i}{G} \dots \dots \dots (15)$$

The gas temperature leaving the i^{th} zone and entering the $i+1^{\text{th}}$ zone is given by the equation:-

$$\int_{\tau_{i-1}}^{\tau_i} \frac{B_g \cdot \epsilon \cdot \rho_g \cdot d\tau}{h_p \cdot a \cdot (t_i - \tau)} = \int_0^{\Delta\theta_i} d\theta \dots \dots \dots (16)$$

Thus by considering the n zones in turn, the temperature history of a band of gas passing through the bed may be calculated, from a knowledge of the solid temperature at each level and the temperature of the gas as it enters the bed.

It may be assumed that the values $\tau_1 \dots \tau_n$ represent the instantaneous gas temperature profile because the total transit time for a band of gas is small compared with the total simulation period.

The solid temperatures $t_1 \dots t_n$ may now be updated after a period $\Delta\phi$ which greatly exceeds the gas transit period for the bed, using the heat balance equation:-

$$t_{i,\theta+\Delta\phi} = t_{i,\theta} + \frac{G \cdot B_g \cdot (\tau_{i-1} - \tau_i) \cdot \Delta\phi}{B_s \cdot (1-\epsilon) \rho_p \cdot \Delta z_i} \dots \dots \dots (17)$$

The repeated use of the above procedure thus enables gas and solid temperatures to be predicted from the initial condition data on the temperature distribution of the solid material forming the bed and the applied gas temperature.

This method was expanded to include fusion, limestone, combustion, drying, the growth of particles during fusion and oxygen concentration. The difference equations used when simulating the test-pot are given in Appendix II.

COMPARISON BETWEEN TEST-POT DATA
AND DIGITAL SIMULATION RESULTS

The accuracy of the digital simulation was verified by comparing test-rig results with simulation results.

The input information for the simulation was mix size, mix density, voidage, coke content, coke size, water content, limestone content, ignition time, ignition temperature and the history of the gas velocity from ignition to burnthrough.

Fig. 2 compares the heat wave leading edge profiles generated by the model and the actual test-pot data. Fig. 2 shows the profiles at 0.076, 0.129 and 0.182 m for a hematite mix with 4.5% coke. The profiles from the model match quite well with the test-pot profiles. Any discrepancies are probably caused by the omission of minor terms from the simulation.

EFFECT OF PROCESS VARIABLES ON HEAT WAVE PROPAGATION
AND THE QUALITY OF SINTER PRODUCED

The model provides a useful means for investigating the effects of manipulating process variables. The manipulation of variables such as air-flow and voidage will have two basic effects; one is to change the heat wave propagation velocity, the other is to change the width of the fusion zone.

The velocity of the heat wave through a sinter bed should be as high as possible if a sinter plant is to produce a maximum output, however if the fusion zone does not produce the right degree of agglomeration there may be a large quantity of rejected sinter and hence a reduced productivity. Too wide a fusion zone will cause large lumps of sinter to form, which will tend to block the passage of air through the bed and hinder the advancement of the heat wave. Too narrow a fusion zone results in a weak fretted structure and a high return fines ratio. The desirable agglomeration conditions probably differ from ore-type to ore-type and also depend upon the lime/silica ratio, however the following simulation results give an insight into the effect of manipulating individual process variables. The authors simulated a 'typical' 0.25m bed. The input data used for calculating the results shown in figures 3-6 are given in Table 1.

Figure No.	3	4	5	5	5	6	6	Units
Ignition temperature	977-1377	1180	1180	1180	1180	1180	1180	°C
Ignition time	40	25-50	40	40	40	40	40	s
Voidage	0.4	0.4	0.4	0.25-0.50	0.4	0.4	0.4	-
Gas inlet velocity	1	1	1	1	0.8-2.0	1	1	m/s
Initial bed temperature	0	0	0	0	0	0	0	°C
Δz , width of zones	0.0025	0.0025	0.0025	0.0025	0.0025	0.0025	0.0025	m
$\Delta \phi$, update period	1	1	1	1	1	1	1	s
Density (return fines and ore)	5000	5000	3500-6000	5000	5000	5000	5000	kg/m ³
Density of coke	1000	1000	1000	1000	1000	1000	1000	kg/m ³
% coke	5	5	5	5	5	3-5.5	5	-
% water	5	5	5	5	5	5	0-18	-
Diameter of particles	0.0030	0.0030	0.0030	0.0030	0.0030	0.0030	0.0030	m

Table 1: Input data used for calculation of results shown in figures 3-6

Temperature of Ignition Gases

Fig. 3 shows the temperature distribution within the bed after 130 seconds, for three different ignition temperatures.

The main points arising from these results are:-

- (i) Propagation of the heat wave is only slightly affected by the ignition temperature.
- (ii) The bed would not ignite at 980°C whilst at temperatures above 1030°C sintering was successfully commenced.

Ignition Period

The effect of longer ignition periods is to slightly widen the fusion zone, Fig. 4. Also the point at which ignition commences is dependent on the ignition time.

Density of Mix, Voidage and Gas Velocity

Fig. 5 shows the effect of changes in voidage, gas velocity and density on burnthrough time. Changes in gas velocity have a very marked effect on heat

wave propagation velocity, whilst voidage and density changes make less though still significant changes to the burnthrough time. Changes to these variables appear to have little effect on the width of the fusion zone.

Coke and Water Content of Mix

Variations in coke and water content whilst not altering the burnthrough time have a marked effect on the width of the fusion zone Fig. 6. When simulating low coke contents (<3.5%) a longer ignition period proved necessary.

Diameter of Mix

Variations in the diameter of the raw mix particles do not affect either the width of the combustion zone or the burnthrough time. However, if the mix is larger than 5mm. ignition will not occur unless the ignition time is increased.

CONCLUSIONS

A model of a sinter bed, based mainly on fundamental relationships, has been formulated and successfully simulated. The model has been validated by comparing heat wave profiles with those from a test-pot. Some initial investigations into the effect of manipulating process variables have been carried out. It was found that variations in burnthrough time (heat wave propagation velocity) during sinter plant operation are mainly caused by changes in gas velocity through the bed. Voidage and density of ore mix are contributory factors. The quality of sinter output will be affected by the proportion of coke in the mix and also by any large deviations in the water content. Ignition time and temperature do not appear to be critical once the minimum time and temperature for ignition have been exceeded.

The methods used are applicable to other problems in macroscopic transport and as such it is hoped that the report will find application outside "sintering".

ACKNOWLEDGEMENT

The authors wish to record their appreciation to the British Steel Corporation for providing access to pilot plant data.

REFERENCES

1. ELLIOTT.J.F., "Some Problems in Macroscopic Transport", Transactions of the Metallurgical Society of A.I.M.E., vol. 227., pp. 802-820, 1963.
2. ROSENBROCK H.H. and STOREY C., "Computational Techniques for Chemical Engineers", Pergamon Press 1966.
3. DASH, I., CARTER, C.E., and ROSE, E., "Heat Wave Propagation Through a Sinter Bed; a critical appraisal of mathematical representations' Proc. SIMAC Conf. on Measurement and Control of Quality in the Steel Industry, Sheffield, Oct. 1974 p8/1 - p8/7.
4. PERRY, R.H. and CHILTON, C.H. 'Chemical Engineers Handbook', Fourth Edition, Mc Graw Hill 1968.
5. PRICE, C. and WASSE, D., 'Relationship Between Sinter Chemistry, Mineralogy and Quality and its Importance in Burden Optimisation'. I.S.I. Publication 152. 1973 pp. 32-52.
6. NYQUIST, O., 'Effects of Lime on the Sintering of Pure Hematite and Magnetite Concentrates', International Symposium on Agglomeration Philadelphia, April 1961, pp. 809-858.
7. BASHFORTH, G.R., 'The Manufacture of Iron and Steel, Vol 1 Chapman and Hall, p. 99, 1960.
8. DENBIGH, K.G. and TURNER, J.C.R., 'Chemical Reactor Theory', Cambridge University Press, 1971.
9. MUCHI, I. and HIGUCHI, J., 'Theoretical Analysis of Sintering Operation', Transactions I.S.I.J. Vol, 12, 1972.
10. ROWE. P.M. and CAXTON, K.T., 'Heat and Mass Transfer from a Single Sphere to Fluid Flowing Through an Array', Transactions Institute of Chemical Engineers, Vol. 43, 1965. pp. T321-T331.
11. PARKER, A.S. and HOTTEL H.C., 'Combustion Rate of Carbon', Ind. and Eng. Chem., 28, 1334, 1936.
12. MIRKO, V.A., KIVIT, G.E. and BURGOV, V.N. 'Analysis of the Gas-Air Regime on a Lengthened Sintering Machine with Sinter Cooling on the Grate Bars', Steel in the U.S.S.R. , Part 2, p.677, 1972.

13. SCHLUTER, R. and BISTRANES, G., 'The Combustion Zone in the Iron Ore Sintering Process.' International Symposium on Agglomeration, Philadelphia, April 1961, pp. 585-637.
14. YAGI, S. and KUNDII, D., 'Combustion of Coke.' 5th International Symposium on Combustion, New York, 1955. p. 231.

APPENDIX I

Formulas that may be used to obtain the important coefficients used in the digital simulation of a sinter test-pot.

Heat and Mass Transfer

The principle mechanism of heat transfer in a sinter bed is by convection. Of the formulas available, (1,8,9,10) for the convective heat transfer coefficient, the following was chosen.

$$\epsilon(N_u) = 2.0 + 0.71 (P_r)^{1/3} (R_e)^{1/2}$$

where

$$N_u = \frac{h d_p}{\lambda}, P_r = \frac{C_g \mu}{k}, R_e = \frac{d_p G}{\mu}$$

A similar formula also exists for the coefficient of mass transfer (K_m) between a gas and particles, in a packed bed.

$$\epsilon(S_h) = 2.0 + 0.71 (S_c)^{1/3} (R_e)^{1/2}$$

where

$$S_h = \frac{K_m d_p}{D}, S_c = \frac{\mu}{\rho_g D}$$

Specific Heat

The specific heat of 'sinter type materials' is given by

$$C_p = 753 + 0.13t$$

A similar relationship exists for sintering gases

$$C_g = 881 + 0.31\tau - 7.98 \cdot 10^{-5} \tau^2$$

Changes in the ratio of O_2 to C_{O_2} have a negligible effect.

Viscosity

The viscosity of sintering gases is given by:-

$$\mu = \mu_0 \left| \frac{\tau}{273} \right|^{3/2} \cdot \left| \frac{386.1}{113+\tau} \right|$$

where $\mu_0 = 1.72 \cdot 10^{-5}$ Kg/ms.

Diffusion Coefficient of O_2 through N_2

The diffusion coefficient is:-

$$D_{ON} = 1.8 \cdot 10^{-5} \cdot \left| \frac{\tau}{273} \right|^n \text{ m}^2/\text{s}$$

where n lies between 1.5 and 2.0

Parker et al (11) suggest a value of 1.5

Coke Combustion

Parker et al (11) have show that K_c , the chemical combustion rate, is given by:-

$$K_c = 6.52 \cdot 10^5 \cdot e^{-18500/Rt} \cdot \sqrt{t}$$

From equation (b) the coefficient of mass transfer is:-

$$\text{Mass transfer } K_m = \frac{D_{ON}}{\epsilon \frac{d}{p}} \left| 2.0 + 0.71(S_c)^{1/3}(R_e)^{1/2} \right|$$

Experimental analyses of sinter bed exhaust have shown that quantities of carbon monoxide are present in the windboxes (9.12,13). The formulae presented above are based on the assumption of complete conversion of coke to carbon dioxide. R. Schluter et al (13) introduce a factor ϕ to modify the mass transfer equation, i.e.

$$K_m = \phi \cdot \frac{D_{ON}}{\frac{d}{p} \epsilon} \left| 2.0 + 0.71 \cdot (S_c)^{1/3}(R_e)^{1/2} \right|$$

Where ϕ is a factor equal to unity for carbon conversion to CO_2 and two for conversion to CO. The CO_2 : CO ratio in the windbox gas is approximately 4:1 where $\phi=1.11$.

It is possible that a layer of ash could surround the particle and hinder combustion but S. Yagi et al (14) suggest that turbulence in the sinter bed would prevent such a layer forming.

APPENDIX II

A cross-section of a partly sintered test-pot yields, from the top to the bottom, the following layer structure. (Fig.1)

- (a) A cooling layer. In this layer the sintered material is convectively cooled by the inlet air.
- (b) A layer of solidification and agglomeration. The combustion of coke lower in the bed causes a certain amount of fusion. In this layer the combustion has ceased and the liquid iron oxides solidify to form sinter.
- (c) A layer in which fusion occurs. The bed is at T_F the fusion temperature. Any remaining heat from uncombusted coke is used for fusion of the iron ore.
- (d) A layer of convective heating and coke combustion. The temperature range in this layer is 1000°K to T_F . 1000°K is the point at which coke combustion commences.
- (e) A convective heating layer. The temperature range of this layer is $373^\circ\text{K} - 1000^\circ\text{K}$.
- (f) Limestone reduction layer. This narrow layer occurs at approximately 870°K . The assumption made by the authors is that the bed temperature remains constant (870°K) within this layer, all available heat being used for the endothermic reduction of limestone.
- (g) A layer of drying. This layer has a temperature of 373°K (boiling point of water) and all available heat is used for vaporisation of water.
- (h) The bottom of the bed is a layer of condensative and convective heating.

The technique outlined in the paper for convective heating, may be expanded to simulate sintering. The bed is divided into a number of vertical zones (typical number 200 zones/m of bed) of width Δz .

The gas transit time through each zone is

$$\Delta\theta_i = \frac{\epsilon \cdot \rho_g}{G} \cdot \Delta z_i$$

The gas temperature is given by the same equation for all parts of the bed:-

$$\int_{\tau_{i-1}}^{\tau_i} \frac{\epsilon \cdot \rho_g \cdot B \cdot d\tau}{h_p \cdot a \cdot (t_i - \tau)} = \int_0^{\Delta\theta_i} d\theta$$

The bed temperature for layers (a) and (e) is:-

$$t_{i,\theta+\Delta\Phi} = t_{i,\theta} + \frac{G \cdot B_g \cdot (\tau_{i-1} - \tau_i) \cdot \Delta\Phi}{B_s \cdot (1-\epsilon) \cdot \rho_p \cdot \Delta z_i}$$

The bed temperature is T_F in layer (b). The heat available for fusion F_u is given by:-

$$F_{u,i,\theta+\Delta\Phi} = F_{u,i,\theta} + G \cdot B_g \cdot (\tau_{i-1} - \tau_i) \cdot \Delta\Phi$$

Similarly for layer (c) the bed temperature is T_F and F_u is given by:-

$$F_{u,i,\theta+\Delta\Phi} = F_{u,i,\theta} + G \cdot B_g \cdot (\tau_{i-1} - \tau_i) \Delta\Phi + \Delta z_i \cdot R_{c_i} \cdot \Delta\Phi H_c$$

In layer (d) the bed temperature is given by:-

$$t_{i,\theta+\Delta\Phi} = t_{i,\theta} + \frac{G \cdot B_g \cdot (\tau_{i-1} - \tau_i) \cdot \Delta\Phi \cdot R_{c_i} \cdot H_c}{B_s \cdot (1-\epsilon) \cdot \rho_p \cdot \Delta z_i} + \frac{G \cdot B_g \cdot (\tau_{i-1} - \tau_i) \cdot \Delta\Phi}{(1-\epsilon) \cdot \rho_p \cdot B_s}$$

Layer (f), limestone reduction. The total heat needed for limestone reduction L_R is given by the product of the mass of limestone in a zone and the heat needed to reduce a unit mass of limestone. The following equation may be used to simulate limestone reduction.

$$L_{R,i,\theta+\Delta\Phi} = L_{R,i,\theta} - G \cdot B_g \cdot (\tau_{i-1} - \tau_i) \cdot \Delta\Phi$$

Layer (g). The rate of removal of water is given by

$$X_{w,i,\theta+\Delta\Phi} = X_{w,i,\theta} - G \cdot B_g \cdot (\tau_{i-1} - \tau_i) \cdot \Delta\Phi / H_v$$

where H_v is the latent heat of vaporization of water, X_w is the mass of water.

Layer (h). The bed temperature is given by

$$t_{i,\theta+\Delta\Phi} = t_{i,\theta} + \frac{G \cdot B_g \cdot (\tau_{i-1} - \tau_i) \cdot \Delta\Phi}{B_s \cdot (1-\epsilon) \cdot \rho_p \cdot \Delta z_i} + \frac{W_{g,i,\theta} \cdot H_v \cdot \Delta\Phi}{B_s \cdot (1-\epsilon) \cdot \rho_p \cdot \Delta\theta_i \cdot \Delta z_i}$$

When the bed reaches the dew point no heat is supplied by the condensation of water vapour. $W_{G_{i,\theta}}$ is the mass of water condensed from the gas during gas transit time $\Delta\theta_i$. The oxygen content at any point in the bed is:-

$$C_{O_{2,i}} = C_{O_{2,i-1}} - R_{c_i} \cdot \Delta\theta_i \cdot \tau_i / 273.3\epsilon$$

$\tau_i / 273.3$ is included so that C_{O_2} is kept at N.T.P. The authors have assumed that there is an increase in the diameter of the input mix caused by the fusion process. This may be justified by the observation, that the gradient of the heating edge is steeper than the gradient of the cooling edge of the heat wave temperature profile. This formula has been adopted for the growth of particles during fusion.

$$d_{F_i} = d_{I_i} \cdot (1 + b \cdot F_{u(\max)_i})$$

where

d_I is diameter of raw mix particles

d_F is final diameter of mix

$F_{u(\max)}$ is maximum heat available for fusion at that point in the bed

b is a constant.

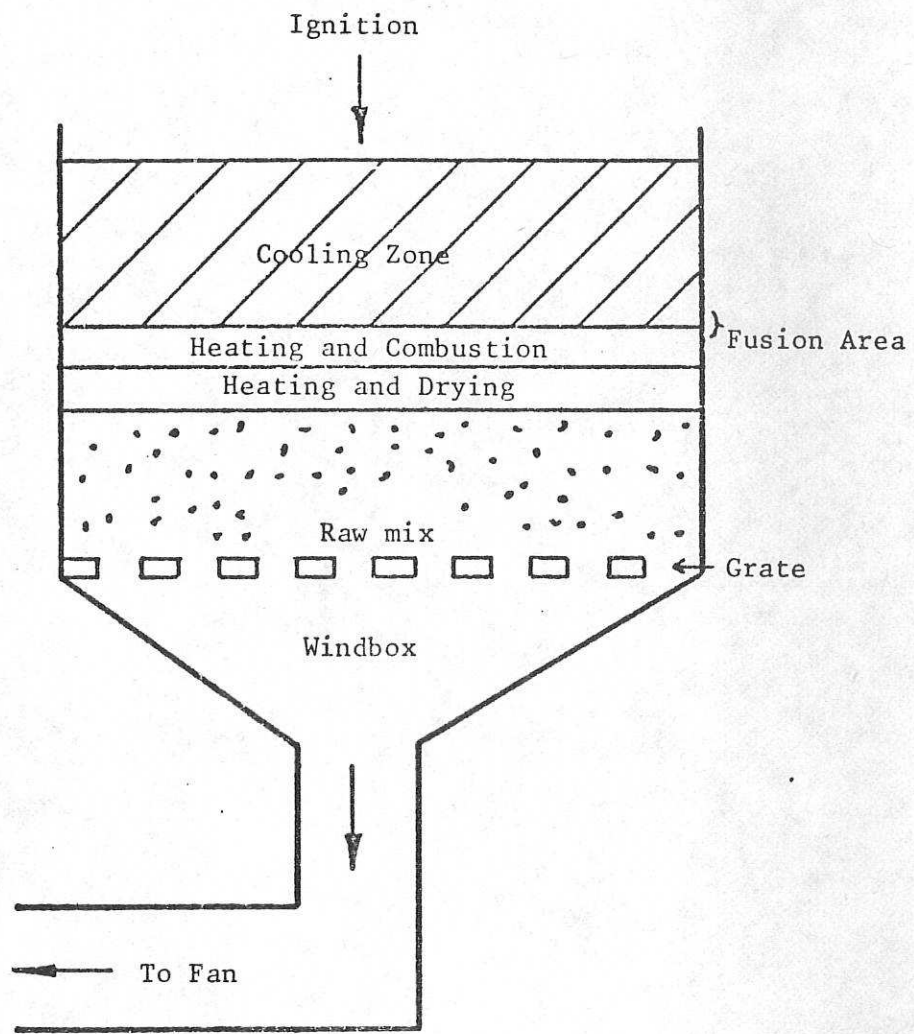


Fig. 1: SINTER TEST-POT AND ZONAL STRUCTURE

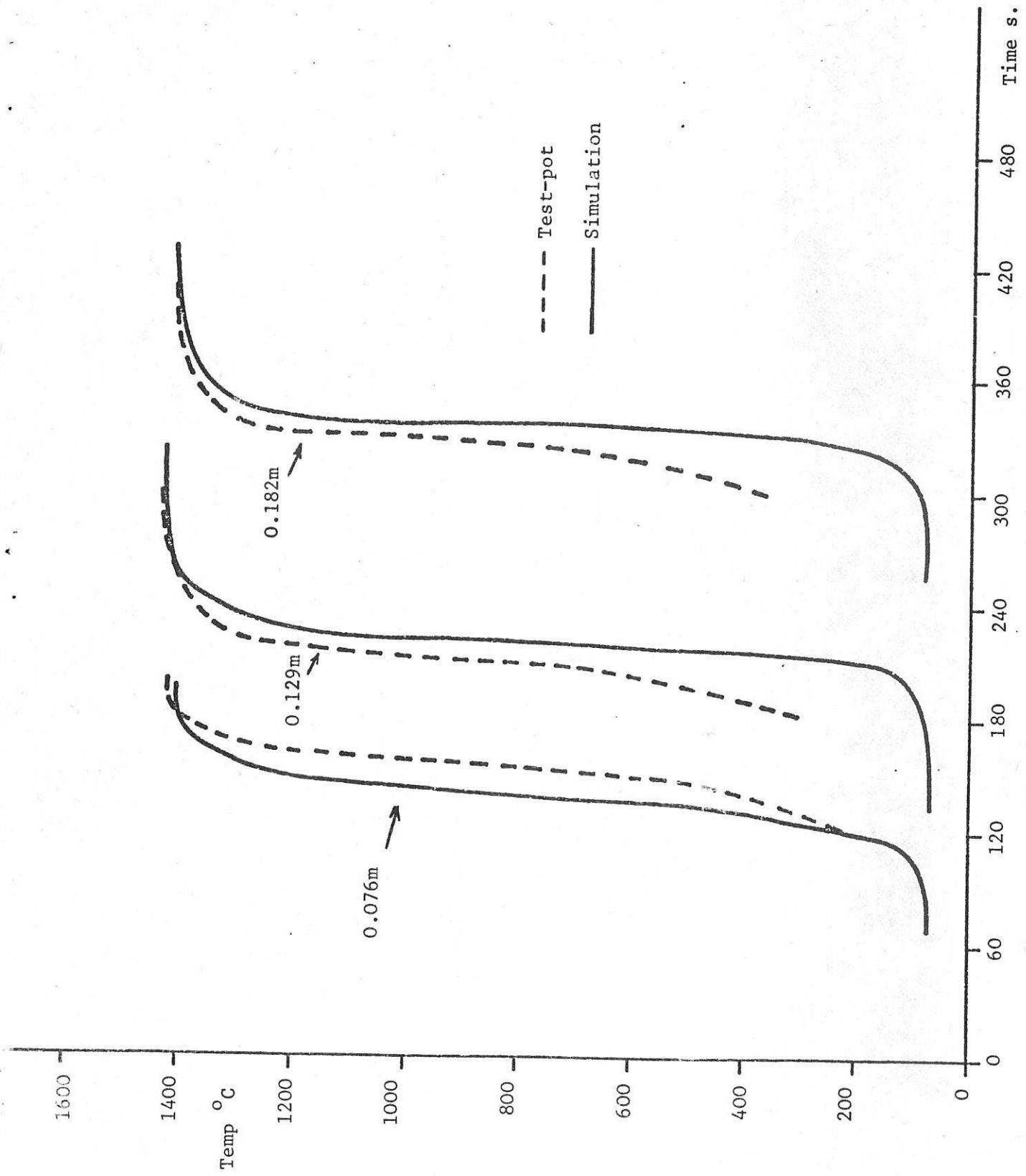


Fig. 2: COMPARISON OF HEAT WAVE FRONT-EDGE PROFILES

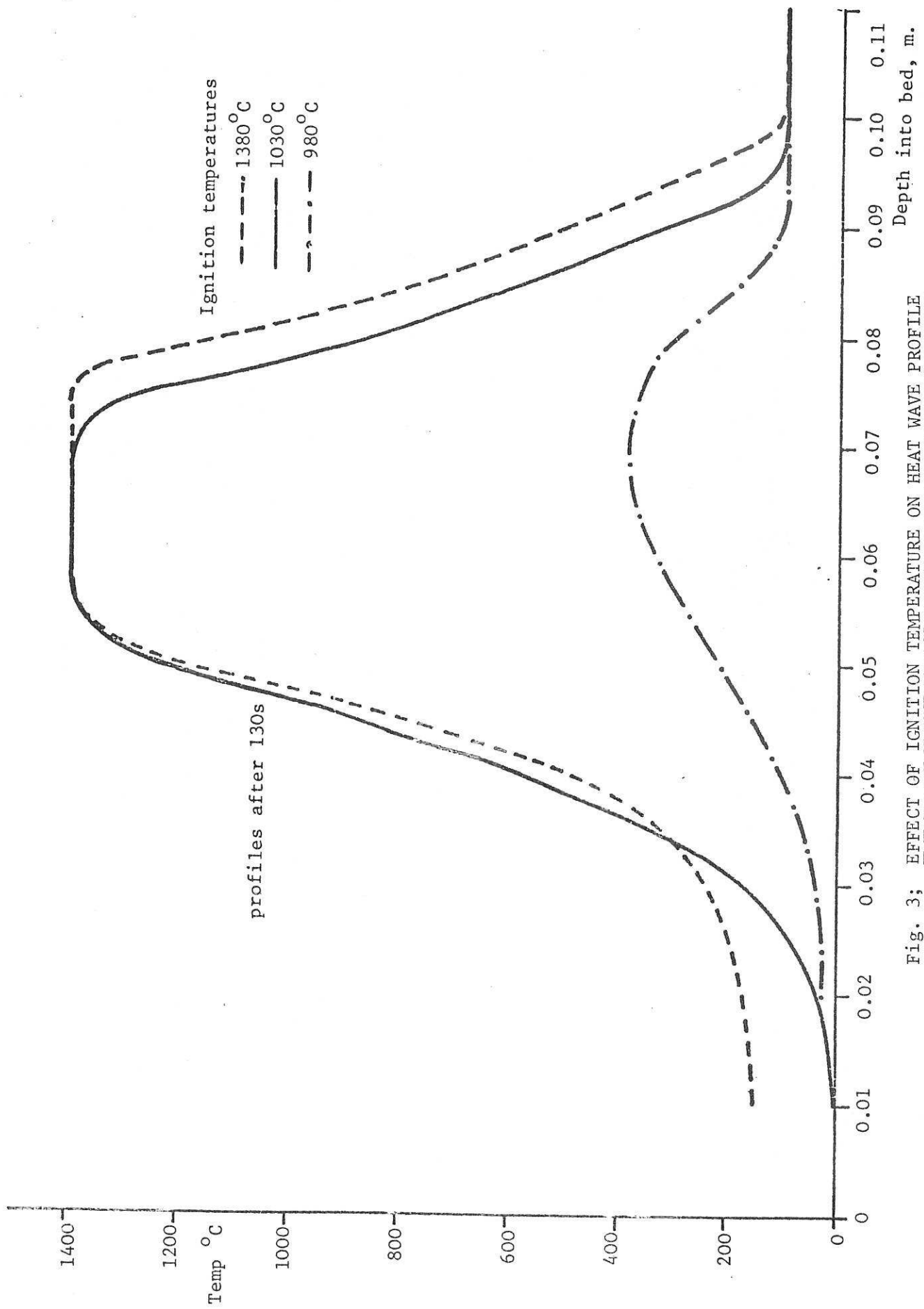


Fig. 3; EFFECT OF IGNITION TEMPERATURE ON HEAT WAVE PROFILE

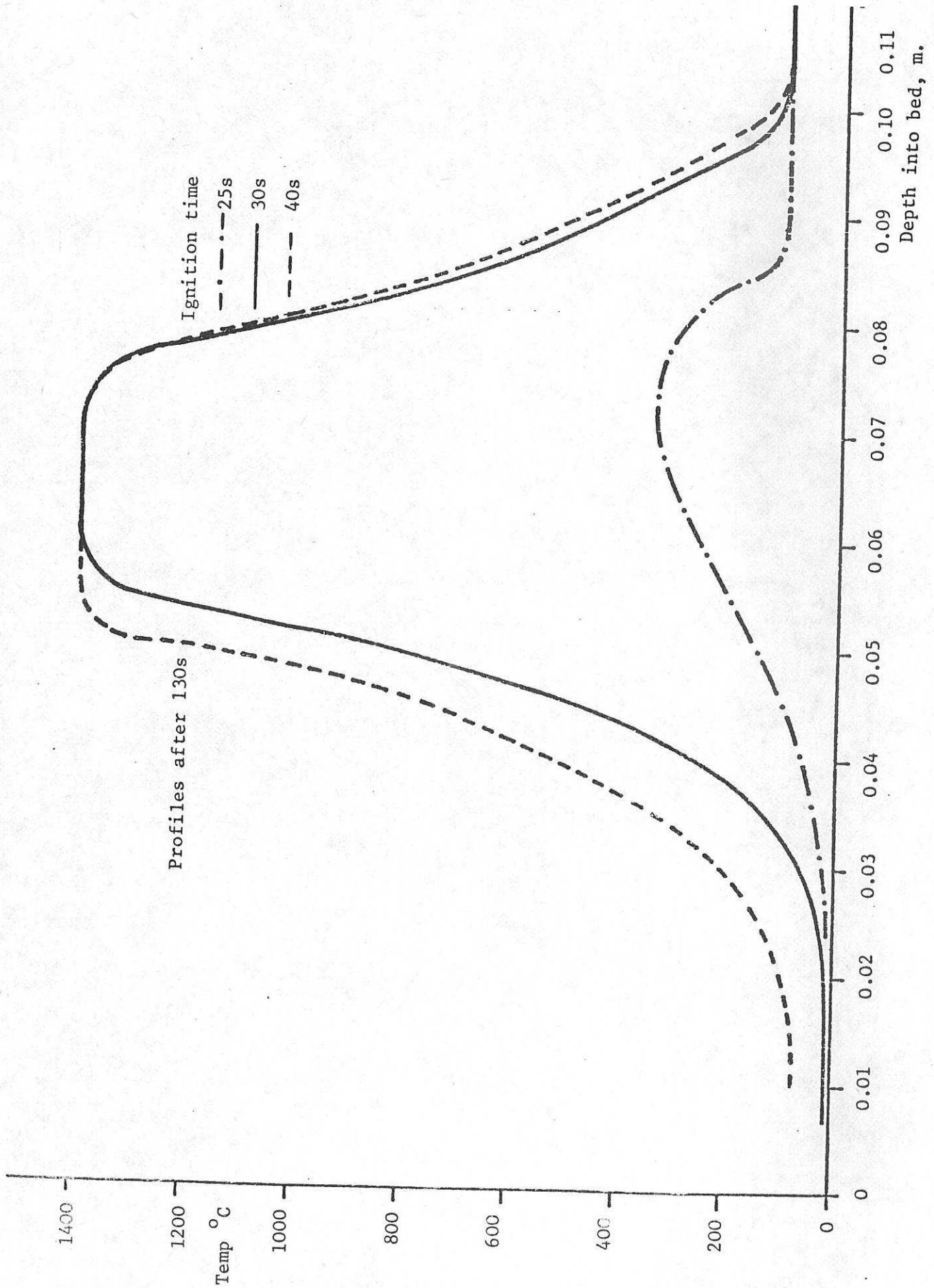


Fig. 4: EFFECT OF IGNITION PERIOD ON HEAT WAVE PROFILE

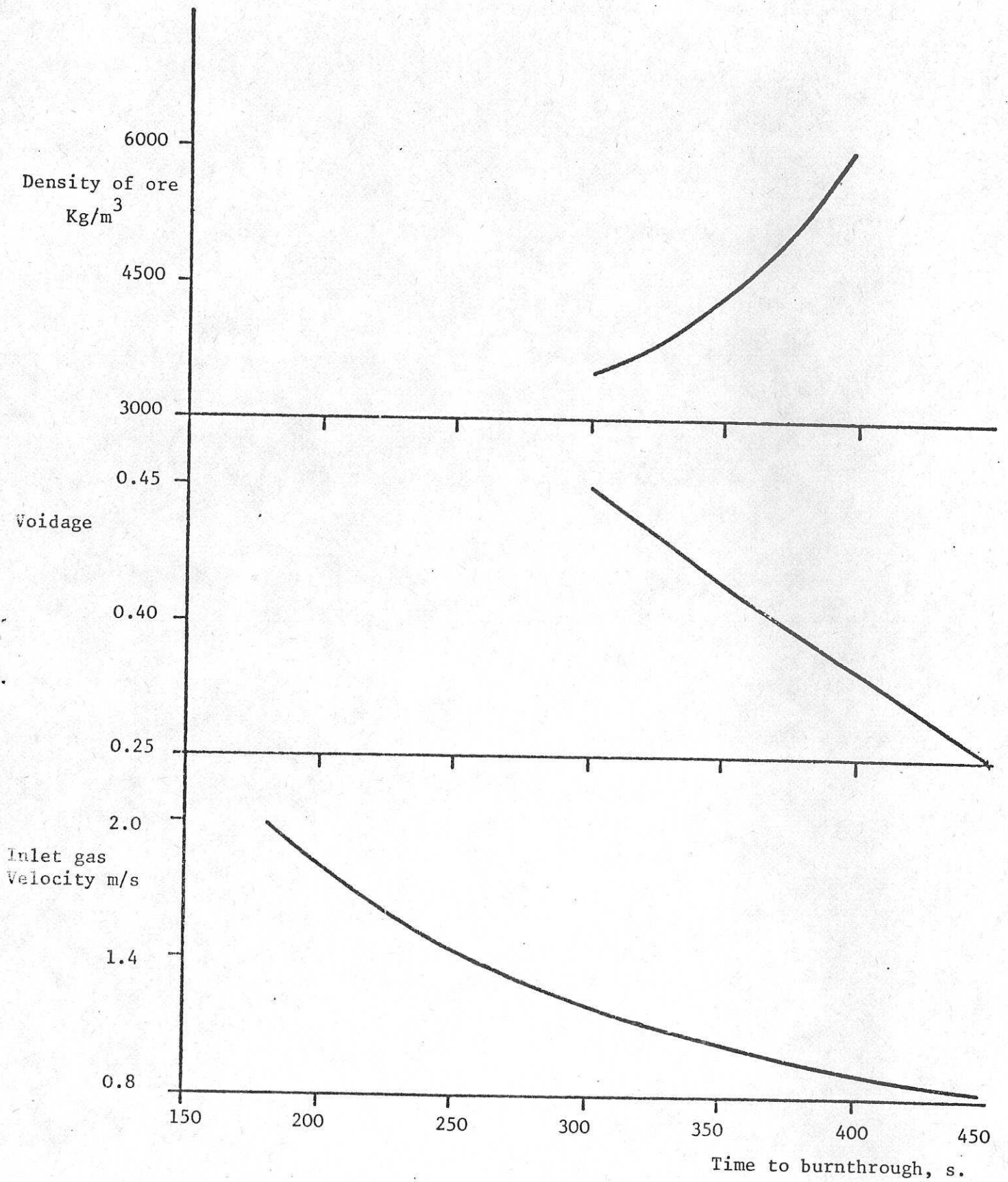


Fig. 5: EFFECT OF DENSITY, VOIDAGE AND GAS VELOCITY ON BURNTHROUGH

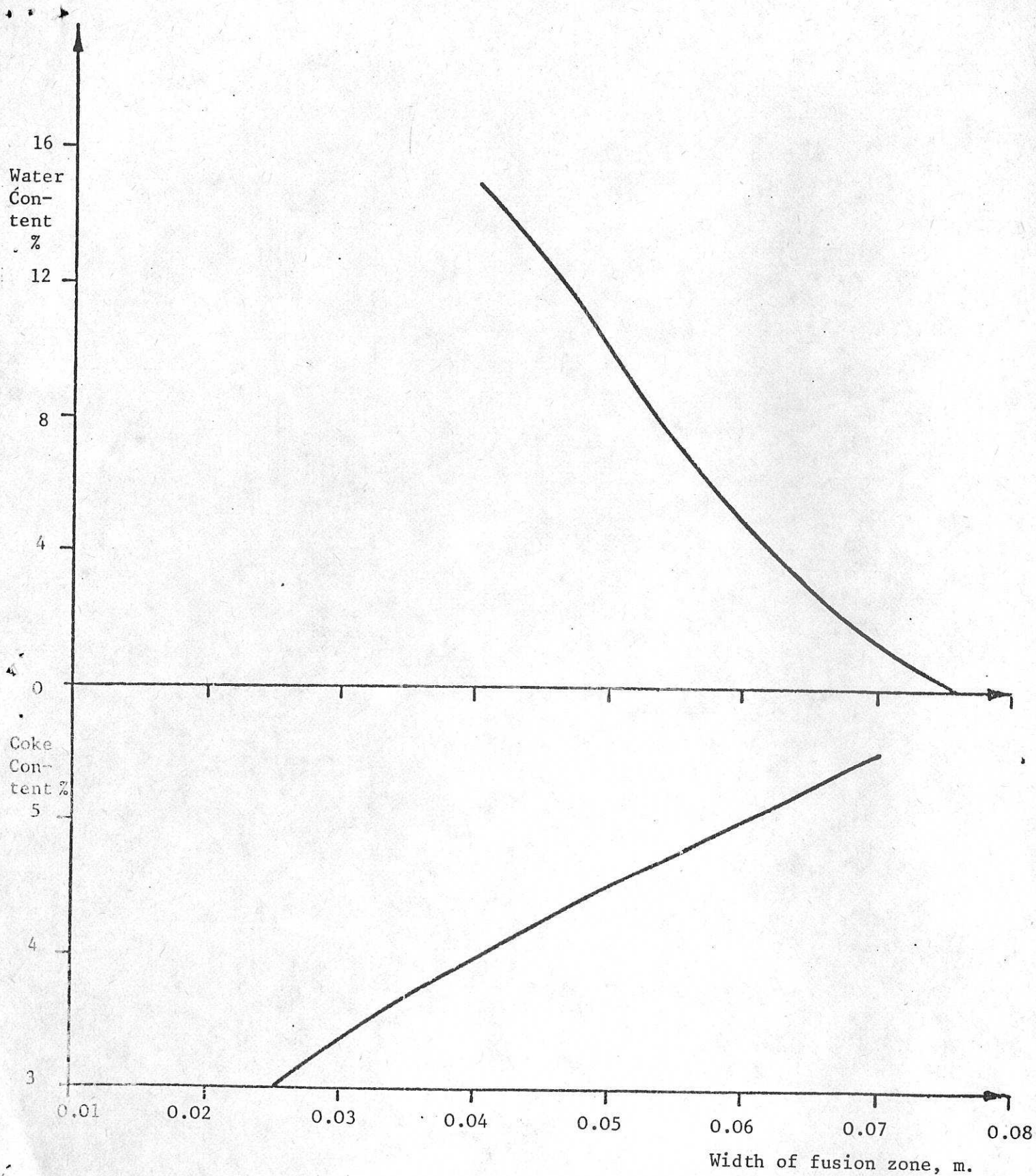


Fig. 6: EFFECT OF COKE AND WATER CONTENT ON WIDTH OF FUSION ZONE